MARTEC™

Smart Solutions for Engineering,
Science and Computing

Probabilistic Reliability and Integrity Assessment of Large Diameter Steel Compliant Risers (SCR) for Ultra-Deepwater Operations: Volume 2 - Reliability Analysis

Martec Technical Report # TR-06-27, Rev 1

June 2006

Prepared for:

Intec Engineering Partnership Ltd.
15600 JFK Boulevard
Houston, TX 77032
USA

Smart Solutions for Engineering,
Science & Computing

Martec Limited
1888 Brunswick Street, Suite 400
Halifax, Nova Scotia B3J 3J8 Canada

tel. 902.425.5101
fax. 902.421.1923
email. info@martec.com
www.martec.com

PROPRIETARY NOTICE

This report was prepared as part of a subcontract from Intec Engineering Partnership Ltd. to Martec Limited (Subcontract No.: 11172601) under the prime contract from the US Minerals Management Services (MMS) (Contract No.: 1435-01-03-RP-74002)

REVISION CONTROL

REVISION	REVISION DATE
TR-06-27	May 30, 2006
TR-06-27, Rev 1	June 30, 2006

SIGNATURE PAGE

Probabilistic Reliability and Integrity Assessment of Large Diameter Steel Compliant Risers (SCR) for Ultra-Deepwater Operations:
Reliability Report

Technical Report # TR-06-27, Rev 1
June 2006

Prepared by: ______________________________ **Date:** ____________________
U.O. Akpan, PhD, P.Eng.
Senior Research Engineer

Prepared by: ______________________________ **Date:** ____________________
P.A. Rushton, MASc
Research Engineer

Prepared by: ______________________________ **Date:** ____________________
T.S. Koko, PhD, P.Eng.
Manager, Emerging Technologies Group

Reviewed by: ______________________________ **Date:** ____________________
T.S. Koko, PhD, P.Eng.
Manager, Emerging Technologies Group

Approved by: ______________________________ **Date:** ____________________
T.S. Koko, PhD, P.Eng.
Manager, Emerging Technologies Group

ACCEPTANCE BY CLIENT

☐ Accepted as is
☐ Accepted subject to change (Details to be provided in attachment.)
☐ Rejected

Client Signature: ______________________________ **Date:** ____________________
Craig Masson
Intec Engineering Partnership, Ltd.

Table of Contents

Table of Figures

List of Tables

EXECUTIVE SUMMARY

The study was aimed at the development of a methodology for assessing the reliability and integrity of large-diameter SCR for ultra-deepwater applications. The study is divided into two parts: Part 1 – deterministic analysis; and Part 2 – probabilistic reliability analyses. A report on the deterministic analysis is presented in a companion document (Volume 1), while this document (Volume 2) is focused on the probabilistic reliability analysis. The primary mode of damage under consideration in this report is fatigue failure. A probabilistic methodology for reliability assessment is developed, which utilises deterministic cumulative fatigue damage indicators namely, the stress levels and cycles associated with the various sea states and the fatigue strength of the members. Specifically, fatigue limit state functions are formulated that use stress levels and stress cycles, and structural strength. Uncertainties in structural load and material properties, which translate into uncertainties in structural responses, are accounted for by assigning probability distributions and standard deviations to the deterministic stress levels. Furthermore, fatigue strength parameters, Miner's indices and capacities, are modelled as random variables. First order reliability and Monte Carlo Simulation solution strategies were employed for estimating fatigue reliability, using the fatigue limit state functions.

The fatigue reliability methodology is applied to three deterministic case studies presented in the companion report (Volume 1). The three case studies involve either a SPAR or a semi-submersible platform. Specifically, the effect of uncertainties in parameters on fatigue reliabilities is investigated for spar hang-off strategies and hull riser tie-in, flexible joint aging and soil pipe interaction. It is noted that the fatigue reliability estimates follow similar trends as the deterministic results. This shows that the probabilistic results can complement deterministic techniques. Additional benefit and insight that is gained from the probabilistic study that can be used for design decisions include information on probabilistic importance factor and probabilistic sensitivity analysis. For the current case studies, it is seen that in general, uncertainties in fatigue strength exponent, *m*, has the highest impact on fatigue reliability of SCR. The second most important random variable is the stress range, *S*, which captures uncertainties in parameters, such as loads, and material properties. These structural and load related uncertainties have been modelled indirectly as random variables due to the lack of a direct reliability capability link in the FEA codes used for fatigue analysis. Parametric sensitivity studies of the fatigue strength parameters indicate that the reliability is sensitive to both the standard deviation and probability distribution of the parameters, thus highlighting the need for accurate probability calibration of the random variables.

1.0 INTRODUCTION

1.1 BACKGROUND

In recent years, offshore reservoirs are being developed in ultra-deepwater environments, where floating production, storage and offloading (FPSO), semi-submersibles and spars are considered to be the most economically viable platforms. Large diameter steel compliant risers (SCR) solutions are being considered for these floating production units in deepwater development such as in the Gulf of Mexico (GOM). Some of the technical challenges which have not been fully addressed include issues such as (i) SCR hang-offs and tie-ins to the hull riser; risk and reliability methodologies for the different hang-off methods (pull tube, flexjoint, stress joint etc) and tie-ins (diver spool, mechanical connectors, etc); (ii) effect of flexible joint aging on weld fatigue at hang-off; (iii) stress recovery and fatigue calculation for vortex-induced vibration (VIV) analysis; (iv) the need for coupled analysis approach in wave-induced fatigue assessment; and (v) effect of soil-pipe interaction on SCR fatigue and extreme responses. A variety of uncertainties are associated with material behavior, environmental loading, hydromechanics modeling, structural modeling, and fatigue/corrosion/wear characteristics, especially at hang-off and tie-in joints. In order to systematically account for such uncertainties, a rational framework is needed.

1.2 OBJECTIVES AND SCOPE

Objectives of the proposed study include the development of a methodology for assessment of the reliability and integrity of large-diameter SCR for ultra-deepwater applications. Effects of fatigue, ageing, and wear associated with terminations at the platform or at sea floor touch-down are included. Methods of accounting for uncertainties in structural, material and environmental parameters are also investigated.

The basic philosophy is to investigate the technical issues identified in Section 1.1, using advanced deterministic methods and tools, within a probabilistic reliability-based framework that systematically accounts for inherent uncertainties. Such an approach will improve the understanding of SCR behavior and design solutions, ultimately leading to more effective management of the risks associated with SCR design. The general approach to be adopted for each of the topics is comprised of the following three steps:

(i) A review and assessment of applicable tools, studies, and data related to the topics;
(ii) Development of improved methodologies and strategies applicable to ultra-deepwater SCR designs;
(iii) Development of a probabilistic reliability-based framework.

Existing approaches for SCR design and analysis are typically based on deterministic methods. Significant effort will be spent on these methods with the aim of improving them for ultra-deep water operations. As improved deterministic design/analysis methods are developed, we will further explore means of introducing uncertainties in model parameters using a probabilistic mechanics approach. The first two steps have been presented in a companion report by INTEC, while the third step, development of a probabilistic reliability framework is the subject of the current report. Specifically, the report is focused on probabilistic framework for fatigue analysis and uses the deterministic results from INTEC studies [1].

1.3 ORGANIZATION OF THIS DOCUMENT

The document is organized as follows. Chapter 2 contains the formulation of a technical approach for fatigue reliability analysis of SCR. The reliability methodology as well as the solution strategy that has been adopted is presented. Application of the fatigue reliability strategy to the various SCR case studies including spar hang-off and hull riser tie-in, effect of flexible joint ageing on SCR semi-submersible hang off with coupled and uncoupled motion and the impact of soil pipe interaction is presented. Summary, conclusion and recommendations as well as the limitations of the methodology are presented in Chapter 4.

2.0 FATIGUE RELIABILITY ANALYSIS APPROACH

2.1 FATIGUE ANALYSIS METHODOLOGY

The procedure employed to evaluate offshore structural fatigue reliability involves three essential steps:

(i) Data collection and characterization, which involves compilation and statistical representation of ocean wave data and other environmental conditions applicable to a particular offshore structural location. This step is the basis for computation of offshore structural loads, which are typically random in nature. For the purposes of this analysis, the calibrated wave, wind, and current data in [1] are employed.

(ii) Computation of structural responses through application of the random loads computed in step (i) to a representative structural model (in this study, the load effects are computed using models developed in [1]).

(iii) The resulting stresses and strains are then used to compute some measure of fatigue damage. Structural reliability is then estimated based on the computed fatigue damage.

Fatigue damage resulting from random or variable amplitude loading is of primary concern here, as this loading is that most applicable to offshore structures. Fatigue damage may be computed using a number of methods. Fundamental to all is the assumption that fatigue behavior (under constant amplitude loading) can be described as some form of the relation

$$N(S)^m = K \tag{1a}$$

where N is the number of stress cycles required to produce fatigue failure at an applied stress level, S denotes the applied stress level, typically described in terms of a stress range (or stress amplitude), and 'K' and 'm' represent the fatigue strength coefficient and fatigue strength exponent, respectively, both empirical material constants. For a specific stress range S_i (i=1,2,3,…,NSR_j, where NSR is the number of applied stress ranges during sea state 'j'):

$$N_i(S_i)^m = K \tag{1b}$$

from which it follows that the corresponding number of cycles to failure is given by

$$N_i = \frac{K}{(S_i)^m} \tag{1c}$$

This relationship is commonly referred to as the 'stress-life' or 'S-N' curve approach. The S-N curve approach is commonly used in conjunction with the Palmgren-Miner rule, a linear damage accumulation rule which suggests that the accumulated damage fraction, D_i, resulting from the application of n_i cycles of stress range S_i is given by

$$D_i = \frac{n_i}{N_i} \tag{2}$$

For applied stresses below a material's endurance limit (S_{end}), it is assumed that damage will be negligible. Consider an offshore structure subjected to loads during a sea state 'j' of timeframe T_j. The total number of applied stress cycles during sea state 'j' is given by $(N_T)_{,j}$, where

$$\left(N_T\right)_j = \sum_{i=1}^{NSR_j} n_i \tag{3}$$

From the above equations, it follows that the total damage accumulated during sea state 'j' is given by

$$D_j = \sum_{i=1}^{NSR_j} D_i = \sum_{i=1}^{NSR_j} \frac{n_i \left(S_i\right)^m}{K} \tag{4a}$$

$$D_j = \frac{1}{K} \sum_{i=1}^{NSR_j} n_i \left(S_i\right)^m = \frac{\left(N_T\right)_j}{K} \sum_{i=1}^{NSR_j} \frac{n_i \left(S_i\right)^m}{\left(N_T\right)_j} \tag{4b}$$

Defining f_i as the probability that a single stress range within sea state 'j' will have magnitude S_i (i.e., the fraction of the total stress cycles of a given sea state that are applied at stress range S_i),

$$\left(f_i\right)_j = \left(\frac{n_i}{N_T}\right)_j \quad , \quad where \sum_{i=1}^{NSR_j} \left(f_i\right)_j = 1 \tag{5}$$

It follows from Equation (4b) that the total damage accumulation during sea state 'j' can also be computed using the following relation

$$D_j = \frac{N_{Tj}}{K} \sum_{i=1}^{NSR_j} \left(f_i\right)_j \left(S_i\right)_j^m \tag{6}$$

The function $\phi = f_i \; \left(i = 1,2,3,\ldots,NSR_j\right)$ essentially defines the probability density curve (or histogram) for the applied stress range associated with each sea state.

For the purposes of this analysis, relevant sea state data for the various structures have been provided, including calibrated significant wave heights, peak periods, wind/current velocities, and durations for a number of individual sea states. Furthermore, a number of critical structural locations (N_{cr}) have been identified for fatigue analysis.

Each relevant sea state will be applied to the structure, resulting in the accumulation of fatigue damage at a given critical location. Damage accumulation due to a single sea state will be computed using the deterministic approach identified by Eq.(6). Typical sea state damage accumulations for a critical location are shown in Table 1.

.

Table 1: Typical Fatigue Damage Accumulation Results

Bin No. 'i'	Avg. of Stress Range, S_i	No. Cycles, N_i	Damage Fraction, D_i
1	1	12780722	1.23E-05
2	3	563555	1.46E-05
3	5	131399	1.58E-05
4	7	122639	4.04E-05
5	9	137239	9.62E-05
6	11	84679	1.08E-04
7	13	49640	1.05E-04
8	15	37960	1.23E-04
9	17	20440	9.66E-05
10	19	14600	9.63E-05
	TOTALS:	13942873	0.000708626
		Fatigue Life (Yrs):	**1411.181639**

The accumulation of fatigue damage throughout a series of relevant sea states is dependent not only on the distribution of applied stresses within each sea state but also on the relative frequency of occurrence of individual sea states. The fatigue damage accumulated at a given structural location within timeframe T_T can thus be expressed as

$$D_{Tot} = \sum_{j=1}^{NSS} p_j D_j = \sum_{j=1}^{NSS} p_j \left(\frac{(N_T)_j}{K} \sum_{i=1}^{NSR_j} (f_i)_j (S_i)_j^m \right) \tag{7}$$

where D_j denotes the damage accumulation during sea state 'j', f_i and S_i (i=1,2,3,…,NSR_j) defines the probability density curve for the applied stresses within each sea state, NSR denotes the number of applied stress ranges associated with each sea state, and T_j represents the duration of sea state 'j' (usually expressed in terms of elapsed time or applied cycles). The probability of occurrence associated with sea state 'j' is denoted by p_j and given by the ratio T_j / T_T, where $T_T = \sum_{j=1}^{NSS} T_j$ (j=1,2,3,…,NSS) and NSS represents the number of relevant sea states.

It is noted that K and m are empirical constants representing the fatigue strength coefficient and exponent (respectively), which may be treated as random variables to reflect the uncertainty in structural capacity, material properties, and the like. It is further noted that the stress S_i (taken here as the average of the applied stress range) is typically randomly distributed due to uncertainties in environmental parameters and structural loading. It is assumed that the fatigue strength parameters (K and m) will remain the same for all selected hot spots.

The various model parameters are recapped below.

K, m = empirical constants representing the fatigue strength coefficient and fatigue strength exponent (respectively), typically used in conjunction with the Palmgren-Miner rule;
NSR_j = the number of applied stress ranges during sea state 'j';
$(S_i)_j$ = the applied stress level corresponding to stress range '*i*' and sea state '*j*';
$(f_i)_j$ = the relative frequency of occurrence for stress range '*i*' of sea state '*j*' (i.e., the fraction of stress ranges or 'blocks' in a given sea state over which constant amplitude stress S_i is acting);
D_j = the fatigue damage accumulated during sea state '*j*';
T_T = overall timeframe for damage accumulation, given by the summation of individual sea state durations T_j;
p_j = the probability of occurrence associated with sea state '*j*'.

2.2 FORMULATION OF REALIABILITY SOLUTION STRATEGY

In this study, the fatigue reliability of the oil and gas risers will be determined using the following limit state function:

$$g(X) = B_R \Delta - B_S D_{Tot} \tag{8a}$$

$$g(X) = B_R \Delta - B_S \sum_{j=1}^{NSS} p_j \left(\frac{(N_T)_j}{K} \sum_{i=1}^{NSR_j} (f_i)_j (S_i)_j^m \right) \tag{8b}$$

where X is the vector of random variables, B_R denotes the modeling uncertainty factor applied to the fatigue resistance limit Δ (also known as Miner's index), and B_S represents the bias factor associated with the fatigue damage calculation itself.

The various assumptions under which the analysis was performed are highlighted below:

- Fatigue damage will be accumulated over a timeframe of 20 years;
- Empirical constants *K* and *m*, representing the fatigue strength coefficient and exponent (respectively) will remain constant for all locations considered, and will be based on the X' S-N curve provided in Volume 1 [1];
- All structural locations will be subjected to the same applied stress ranges;
- The Flexcom-3D/LifeTime fatigue predictions are presented in a format such that the sea state probabilities are already built into the histogram of applied stresses at each critical location. As such, the analysis can be treated as having a single sea state (i.e., NSS=1).

Equation (8b) indicates that there are 6 basic random variables used in this limit state function: B_R, Δ, B_S, *m*, *K*, and S_i. However, for the purposes of this analysis, the applied stress data supplied in volume 1 [1] was discretized into stress ranges and cycles that affect cumulative damage ($\sigma \in [0,150] MPa$), resulting in a larger number of random variables (about 95 – 152 variables).

Once the limit state function has been defined, the reliability of offshore structural components can be defined as the likelihood of their functioning according to their designed purpose for a particular time period (e.g., an intended service life). Reliability methods exist for computing instantaneous reliability of structural components. Some of the most commonly applied techniques will be discussed in the following paragraphs.

The instantaneous reliability of an SCR structural component/subsystem, such as the riser system, may be computed using a limit state or performance function ($g(X)$) defined in terms of a failure mode of interest (e.g., fatigue, buckling, corrosion, etc). The failure domain (Ω) is defined by a negative performance function (i.e., $\Omega = \left[g\left(X\left(t\right)\right) < 0\right]$), while its compliment ($\Omega^{'} = \left[g\left(X\left(t\right)\right) > 0\right]$) defines the safe region. The instantaneous failure probability at time t is defined as

$$P_f\left(t\right) = \int_{\Omega} f\left(X\left(t\right)\right) dX \tag{9}$$

where $f(X(t))$denotes the joint probability density function of the basic random variables (X) at time t. As the joint probability density function is generally unknown, evaluation of this convolution integral becomes a rather difficult task. Several practical approaches have been developed, including first-order reliability methods (FORM) and second-order reliability methods (SORM).

First-Order Reliability Methods (FORM), also known as Fast Probability Integration (FPI) Schemes, are the most robust methodologies for computing instantaneous failure probability. The method uses the Hasofer-Lind (or H-L) formulation (or Advanced First Order Second Moment (AFOSM) model), the basic concept of which involves the transformation of Gaussian (i.e., normal) random variables to the standard form (i.e., with zero mean and unit standard deviation). The Hasofer-Lind reliability index, denoted by β_{HL}, is then computed as the minimum distance from the origin to the limit state surface. Although the H-L formulation is limited to cases involving Gaussian variables, the work represents an important milestone and has laid a solid foundation for the development of a class of procedures generically referred to as first-order reliability methods (FORM). FORM procedures are essentially optimization-based techniques that are used to evaluate the reliability index (β), from which the failure probability (P_f) can be computed using the following relationship:

$$\beta = \Phi^{-1}\left(P_f\right) \tag{10}$$

where Φ denotes the standard normal cumulative distribution function (CDF). FORM procedures utilize the full distribution information for all random variables included in the limit state function. Correlation between the random variables is permitted with FORM. Several techniques are available with which to complete FORM calculations. It is sufficient, however, to illustrate the basic features of the entire class via a description of a particular scheme called the HL-RF algorithm. This algorithm is named after Hasofer and Lind [2], based on the work described above, and Rackwitz and Fiessler [3], who first proposed the generalization of the H-L scheme to non-Gaussian random variables. The Hasofer-Lind and Rackwiz-Fisseler (HL-RF) algorithm has become one of the most popular FORM procedures employed today.

The essential steps involved in FORM algorithms include:

(i) a transformation of the vector of basic random variables from the original *X*-space to the standard normal *u*-space;

(ii) a search (usually in u-space) for the point (u^*) on the limit state surface (i.e., $g(u)=0$) that has the highest joint probability density. This point is commonly referred to as the design point, failure point, or the most probable point (MPP);

(iii) an approximation of the failure surface (in *u*-space) at the MPP; and

(iv) a computation of the distance from the origin to the MPP, referred to as the reliability index (β). This information can then be used to compute the associated failure probability (P_f).

The transformation from the original *X*-space to standard normal *u*-space is usually denoted by the transformation operator (T), such that:

$$U = T(X) \tag{11}$$

This probability transformation scheme has been verified to yield extremely accurate results in reliability analysis. The search for the most probable point is conducted via solution of an optimization problem. The optimization problem pertaining to the calculation of the Hasofer-Lind reliability index in *u*-space may be summarized as follows:

$$\begin{aligned} &minimize\ \ D = \sqrt{u_i^T u_i} = \beta \\ &subject\ to\ \ g(u_i) = 0 \end{aligned} \tag{12}$$

The solution of this problem locates the MPP and the n-dimensional position vector locating this point (U^*) is given by

$$U^* = \alpha^* \beta \tag{13}$$

where α^* denotes the unit normal vector at the MPP. That is,

$$\alpha^* = \frac{\nabla g(U^*)}{|\nabla g(U^*)|} \tag{14}$$

in which ∇ represents the gradient operator. First Order Reliability Methods assume a linear approximation of the performance function at the MPP. The computed reliability index (β) has a one-to-one non-linear relationship with the failure probability.

The HL-RF algorithm is currently the most widely used method for solving the constrained optimization problem in structural reliability (Lui and Der Kiureghian, [4]). The method is based on the following recursive formula:

$$U_{k+1} = \frac{1}{\nabla g^T(U_k)\nabla g(U_k)}\left(\nabla g^T(U_k)U_k - g(U_k)\right)\nabla g(U_k) \tag{15}$$

Experience shows that for most situations, the HL-RF algorithm converges rapidly. Alternatively, the Monte Carlo Simulation (MCS) technique, in which the failure set, g(*X*), is populated through generation of random samples, has proven to be a valuable instrument in reliability analysis. These capabilities are available in Martec's general-purpose reliability analysis tool COMPASS (Orisamolu et al, [5]), which is used for the reliability analysis in this study.

3.0 RELIABILITY ANALYSIS OF CASE STUDIES

3.1 SPAR HANG-OFF STRATEGIES AND HULL RISER TIE-IN

3.1.1 Problem Description

The generic spar model for use in 10000 feet water depth in the Gulf of Mexico, presented in Chapter 4 of the Volume 1 report by INTEC [1], is used for reliability analysis. A detailed description of the problem configuration is provided in [1]. For completeness a summary of the Hull, and Riser data are provided in Table 2, and Table 3. The purpose of this case study is to investigate fatigue reliability associated with various hang-off locations as well as the hang-off connections. Based on the deterministic fatigue results [1], uncertainties are assigned to the random variables, which are employed in a probabilistic fatigue analysis.

Table 2: SPAR Hull Data [1]

Item	Value	Unit
Hull Geometry		
Displacement	118099 \ 53550	kip \ Te
Draft	500.3 \ 152.5	ft \ m
Hard tank diameter	115 \ 35	ft \ m
Hard tank height	233 \ 71	ft \ m
Free board	50.8 \ 15.5	ft \ m
Truss height	300.2 \ 91.5	ft \ m
Soft tank height	18.0 \ 5.5	ft \ m
Soft tank width/breadth	81.4 \ 24.8	ft \ m
Center-well width/breadth	49.2 \ 15	ft \ m
Truss Configuration		
Truss column diameter	8.2 \ 2.5	ft \ m
Number of heave plates	3	-
Heave plate OD	114.8 \ 35	ft \ m
Mooring Configuration		
Number of mooring line groups	4	-
Number of mooring lines	16	-
Fairlead hang-off elevation	318 \ 97	ft \ m (above keel)
Riser configuration		
Number of SCRs	2	-
SCR hang-off elevation (Option 1 – soft tank)	18.0 \ 5.5	ft \ m (above keel)
SCR hang-off elevation (Option 2 – hard tank)	318 \ 97	ft \ m (above keel)
Topside Weights		
Max. topside weight in extreme condition	30190 \ 13690	kip \ Te
Deck VCG in extreme condition (from keel)	617 \ 188	ft \ m
Max. topside weight in operating condition	30680 \ 13910	kip \ Te
Deck VCG in operation condition (from keel)	620 \ 189	ft \ m

The SCR hang-off locations are given in

Table 3. The coordinate system is shown in Figure 1. The origin is located at the keel at the platform center with the z-coordinate upwards. There are two alternative hang-off options: soft tank and hard tank. In both cases the x and y coordinates of the hang-off locations are the same. There is a 3-meter separation between the hang-off points, and the riser headings differ by 5 degrees.

Table 3: SCR Hang-Off Details [1]

Hang-Off Option	**X (ft \ m)**	**Y (ft \ m)**	**Z (ft \ m)**	**Azimuth Angle wrt X-axis (degree)**
Option 1 – Soft Tank				
Gas riser	37.7 \ 11.5	59.0 \ 18.0	18.0 \ 5.5	50
Oil riser	47.6 \ 14.5	59.0 \ 18.0	18.0 \ 5.5	45
Option 2 – Hard Tank				
Gas riser	37.7 \ 11.5	59.0 \ 18.0	318.2 \ 97	50
Oil riser	47.6 \ 14.5	59.0 \ 18.0	318.2 \ 97	45

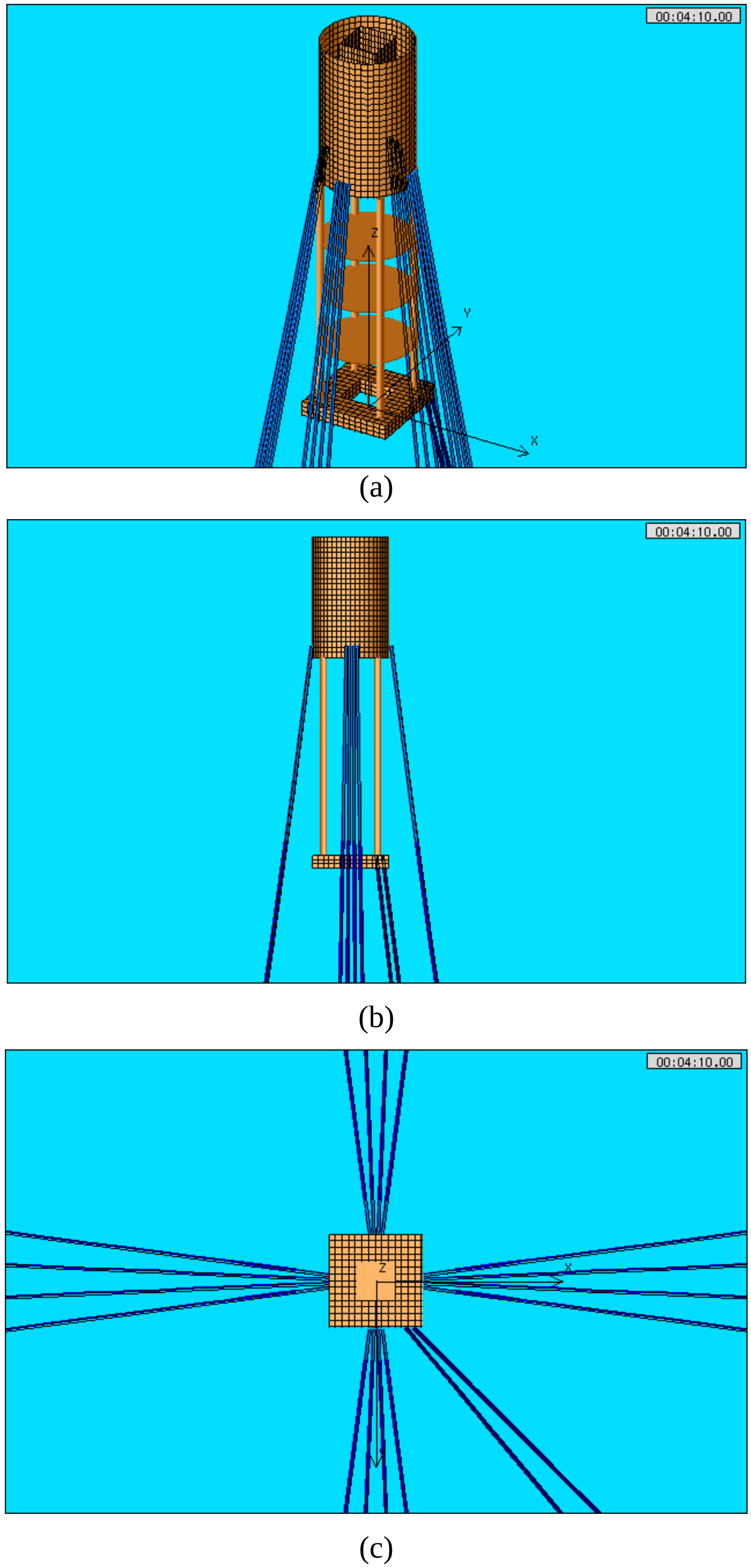

Figure 1: SPAR Model (a) Isometric View; (b) Elevation View; (c) Bottom View [1]

3.1.2 Reliability Analysis

The total number of random variables used for the reliability analysis was 152 and are summarized in Table 4.

Table 4: Description of Random Variables Used in the Reliability Analysis (Hang-off Strategies)

Variable Name	Mean Value	Coefficient of Variation	Probability Distribution
DELTA	1.000	0.25	Weibull
BR	1.000	0.25	Weibull
BS	1.000	0.25	Lognormal
S-N_m	3.740	0.10	Lognormal
S-N_K	2.50E+13	0.10	Lognormal
Fatigue Stress Levels (MPa)	0.25 0.75 1.5-59.5 in 1.0 increments 61.0-99.0 in 2.0 increments 102.5.0-147.5 in 5.0 increments 155.0-195.0 in 10.0 increments 210.0-290.0 in 20.0 increments 325.0-575.0 in 50.0 increments	0.4	Gumbel

The various structural hot spots considered were grouped according to the following categories [1] :

- Hard Tank
  - Gas Riser
    - Hang-Off
    - Touch-Down Points 1-13
  - Oil Riser
    - Hang-Off
    - Touch-Down Points 1-13
- Soft Tank
  - Gas Riser
    - Hang-Off
    - Touch-Down Points 1-13
  - Oil Riser
    - Hang-Off
    - Touch-Down Points 1-13

All reliability analyses were carried out based on the First-Order Reliability Method (FORM), the results of which are presented in Table 5 (Note: the following abbreviations apply: HT=hard tank; ST=soft tank; GR=gas riser; OR=oil riser; X=S-N curve ‘X’; and TDP=touch down point).

For some structural locations considered, failure probabilities were too low, that is, essentially zero. Only those locations for which failure probability, $P_f \geq 1\text{x}10^{-5}$ are presented in the table below.

Table 5: Probabilistic Reliability Analysis Results (Hang-off Strategies)

Load Case Description	Location	Element / Stress Point	Cumulative Damage	Reliability Index	Failure Probability
HT/GR/X	G1610 Hangoff	E632-SP1	2.279E-04	3.302	4.803E-04
HT/GR/X	G1610 Hangoff	E632-SP7	6.810E-05	3.996	3.220E-05
HT/GR/X	G1610 Hangoff	E631-SP7	5.626E-05	4.223	1.204E-05
HT/GR/X	G1610 Hangoff	E630-SP7	4.637E-05	4.258	1.028E-05
HT/OR/X	O1610 Hangoff	E632-SP1	2.930E-04	3.177	7.439E-04
HT/OR/X	O1610 Hangoff	E632-SP7	7.445E-05	3.997	3.200E-05
HT/OR/X	O1610 Hangoff	E631-SP7	6.071E-05	4.121	1.885E-05
ST/GR/X	G1610 Hangoff	E632-SP1	2.054E-04	3.308	4.707E-04
ST/GR/X	G1610 Hangoff	E632-SP3	1.002E-04	3.739	9.222E-05
ST/GR/X	G1610 Hangoff	E631-SP3	8.323E-05	3.782	7.790E-05
ST/GR/X	G1610 Hangoff	E630-SP3	6.907E-05	3.870	5.433E-05
ST/GR/X	G1610 Hangoff	E629-SP3	5.741E-05	4.180	1.456E-05
ST/GR/X	G1610 Hangoff	E628-SP3	4.585E-05	4.200	1.331E-05
ST/OR/X	O1610 Hangoff	E632-SP1	2.103E-04	3.314	4.606E-04
ST/OR/X	O1610 Hangoff	E632-SP3	8.459E-05	3.838	6.199E-05
ST/OR/X	O1610 Hangoff	E631-SP3	6.810E-05	3.985	3.373E-05
ST/OR/X	O1610 Hangoff	E630-SP3	5.456E-05	4.119	1.900E-05
ST/OR/X	O1610 Hangoff	E629-SP3	4.350E-05	4.205	1.304E-05

The results for all locations (including those not presented in Table 5) are consistent with INTEC's findings, suggesting that the hang-off region is consistently the most critical in terms of fatigue. The long fatigue lives predicted by the Flexcom-3D/LifeTime software are supported by the high reliability indices computed during the probabilistic analysis. A review of the parametric importance factors predicted by the probabilistic analysis suggests that the fatigue strength exponent (i.e., slope of the S-N curve) 'm' and stress range 'S_i', respectively, are the two parameters whose uncertainty (indicated by their respective COVs) most affects riser reliability, followed by the modeling uncertainty parameter B_R and Miner's index Δ (which generally exhibit an equal importance) and finally the bias factor B_S. It should be noted that in reality, it is expected that 'K' and 'm' will be correlated random variables, and should therefore exhibit a comparable level of importance. The pie chart in Figure 2 depicts typical results for the distribution of parametric uncertainty importance at two locations (HT/OR/X-E632-SP7 and HT/OR/X-E632-SP1. See Table 5)

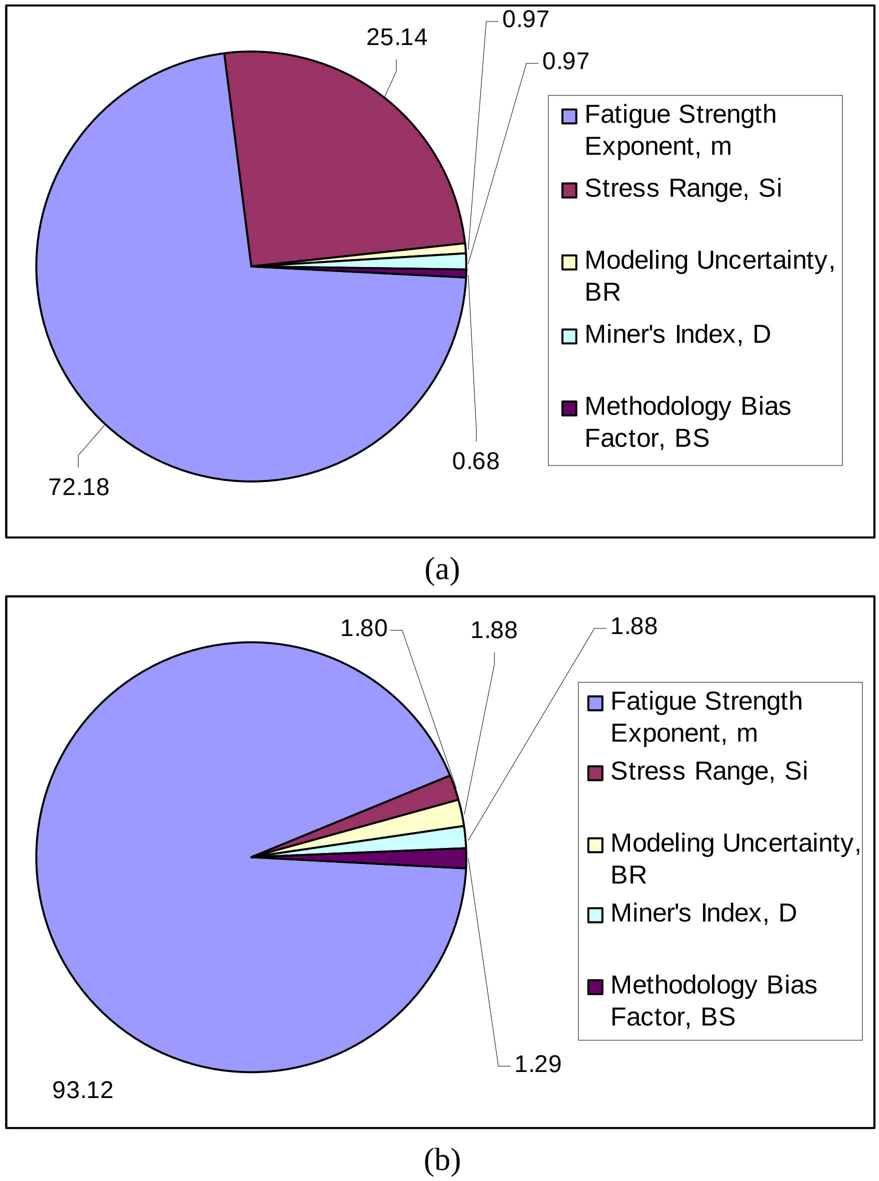

Figure 2: Distribution of Importance Factors for the Random Variables (a) HT/OR/X – E632-SP7; (b) HT/OR/X – E632-SP1

It is interesting to note that reliability and the relative importance of the basic random variables (B_R, Δ, B_S, m, K, and S_i) is strongly a function of the randomness of the fatigue strength exponent '*m*'. For example, when only '*m*' is considered deterministic, structural reliability increases dramatically, with B_R and Δ becoming the most important parameters. Therefore, efforts should be directed toward adequate calibration of 'm' for the various materials at the locations of interest. Since stress range S_i is a function of sea state statistics, close attention should also be paid to the calibration of this variable. Uncertainties in both '*m*' and 'S_i' will impact on the accuracy of both deterministic and probabilistic results.

To illustrate the parametric importance of the fatigue strength exponent '*m*', a sensitivity study was conducted, in which its original probabilistic characteristics were modified and the resulting impact on reliability noted. The results are summarized in Figure 3, Figure 4 and Figure 5. One of the most critical hot-spot locations (Hard Tank – Oil Riser – E632-SP7, (see highlighted location in Table 5) was selected for this demonstration.

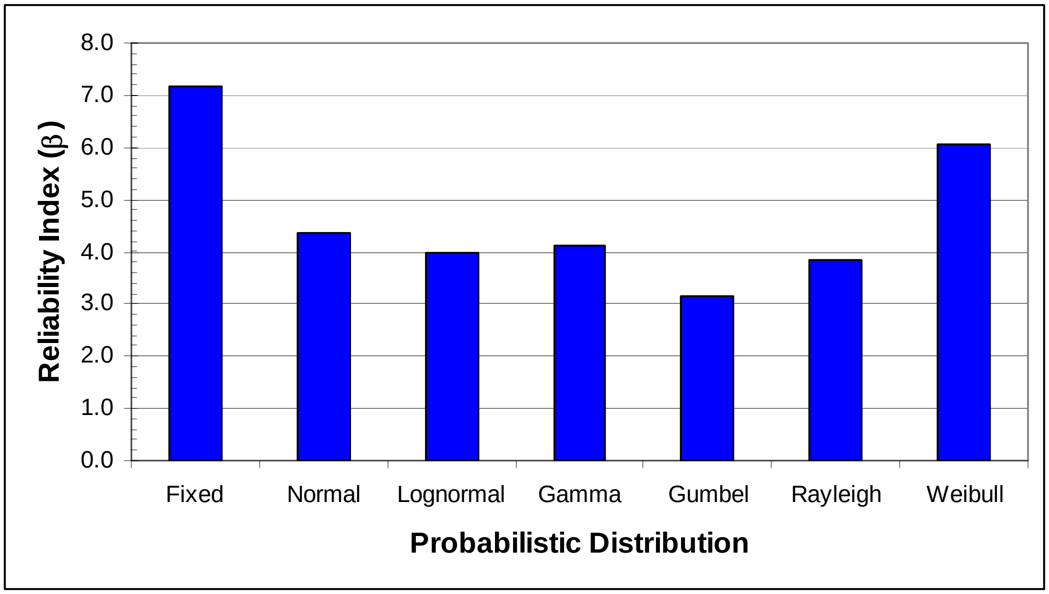

Figure 3: Reliability Index as a Function of Probabilistic Distribution of Fatigue Strength Exponent '*m*' (HT/OR/X – O1610 Hang-Off)

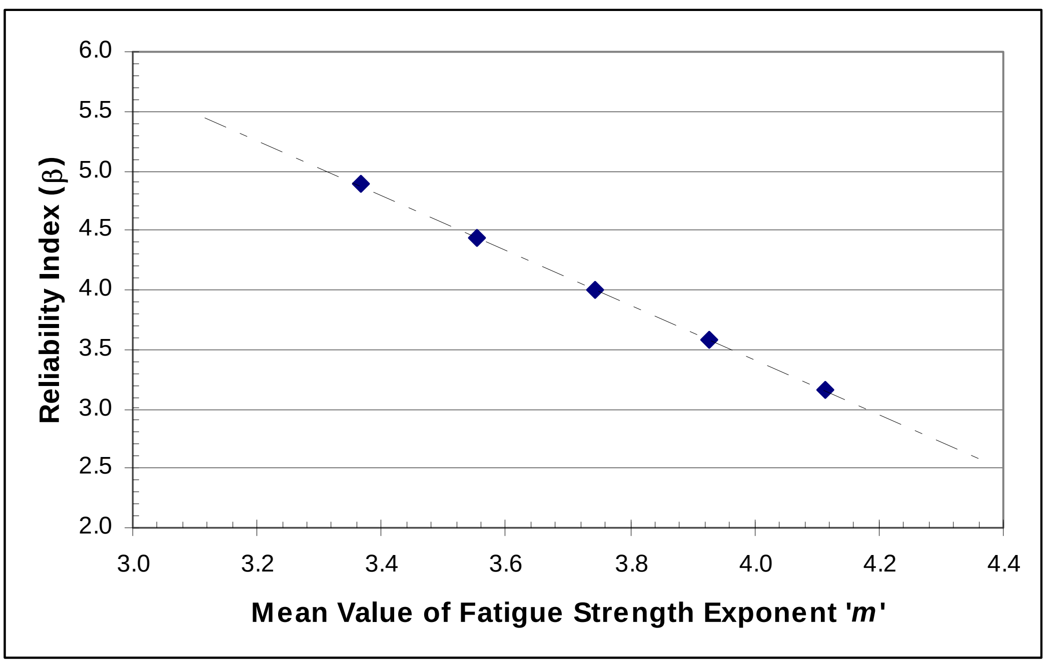

Figure 4: Reliability Index as a Function of Mean Value of Fatigue Strength Exponent '*m*' (HT/OR/X – O1610 Hang-Off)

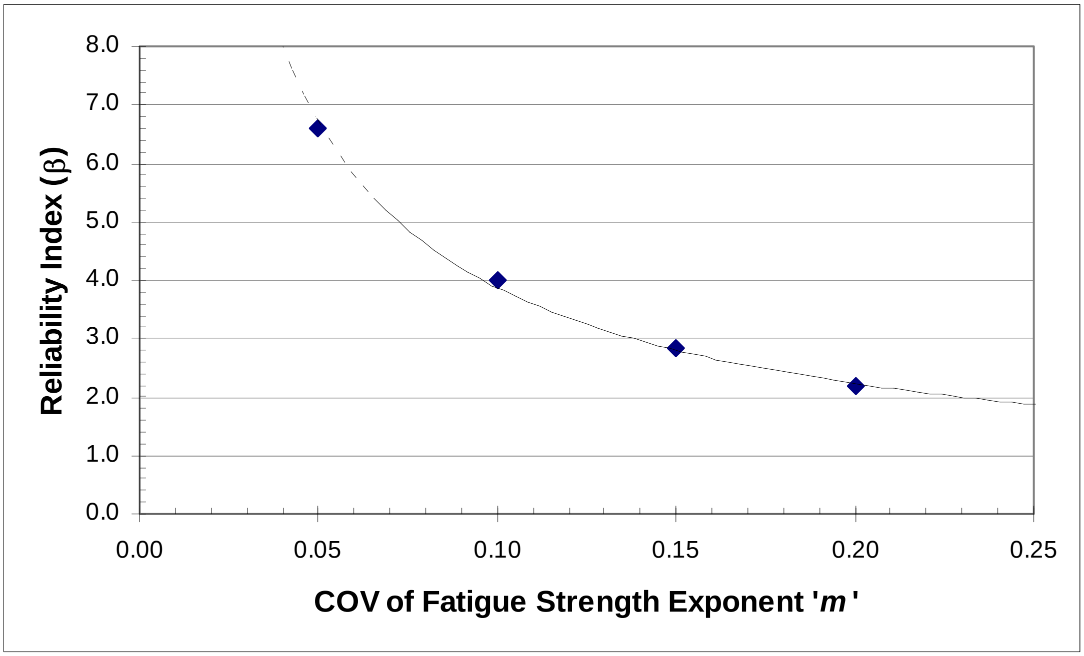

Figure 5: Reliability Index as a Function of COV of Fatigue Strength Exponent '*m*' (HT/OR/X – O1610 Hang-Off)

3.2 EFFECT OF SCR FATIGUE UNDER COUPLED AND UNCOUPLED MOTION; AND EFFECT OF FLEXIBLE JOINT AGEING ON SCR HANG-OFF

3.2.1 Problem Description

Fatigue is a primary design consideration for SCRs. Typically, there are two most critical fatigue hot spot areas in an SCR, one at the touchdown point (TDP) at the seabed, and the other at the hang-off to the host platform. For a hang-off system utilizing a flexible joint, the fatigue life of the weld just below the flexible joint is directly affected by the rotational stiffness of the flexible joints. Higher stiffness leads to higher bending stress in the weld, and hence higher fatigue damage. The key component of a flexible joint is the flexible element, which is made of special elastomeric material supported by metal inserts. As the elastomer ages, its property may change and may potentially lead to stiffening of the flexible joint.

The generic four-column semi-submersible hull with a ring-pontoon and an operational draft 0f 33.5 m and the corresponding displacement of 45.000.0 t, presented in Chapter 4 of the Volume 1 [1], is used for reliability analysis. A detailed description of the problem configuration is provided in [1]. For completeness a summary of the Hull, and Riser data are provided in Table 6 and Figure 6. The purpose of this case study is to investigate fatigue reliability under coupled and uncoupled motion, and flexible joint ageing on SCR hang-off connections. Based on the deterministic fatigue results [1], uncertainties are assigned to the random variables, which are employed in a probabilistic fatigue analysis.

Table 6: Semi-Submersible Hull Data [1]

Item	Value	Unit
Hull Geometry		
Displacement	98910 \ 44850	kip \ Te
Draft	109.9 \ 33.50	ft \ m
Hull height	165 \ 50.29	ft \ m
Hull width and breadth	247.7 \ 75.50	ft \ m
Column width and breadth	46.75 \ 14.25	ft \ m
Pontoon length	154.2 \ 47.00	ft \ m
Pontoon breadth	36.1 \ 11.00	ft \ m
Pontoon height	26.2 \ 8.00	ft \ m
GM (Meta-center height above center-of-gravity)	18.0 \ 5.50	ft \ m
KM (Meta-center height above keel)	97.3 \ 29.65	ft \ m
Mooring Configuration		
Number of mooring line groups	4	-
Number of mooring lines	12	-
Riser configuration		
Number of SCRs	2	-
SCR hang-off elevation	13.1 \ 4	ft \ m (above keel)
Topside Weights		
Max. topside weight in extreme condition	30190 \ 13690	kip \ Te
Deck VCG in extreme condition (from keel)	226.4 \ 69	ft \ m
Max. topside weight in operating condition	30680 \ 13910	kip \ Te
Deck VCG in operation condition (from keel)	229.7 \ 70	ft \ m

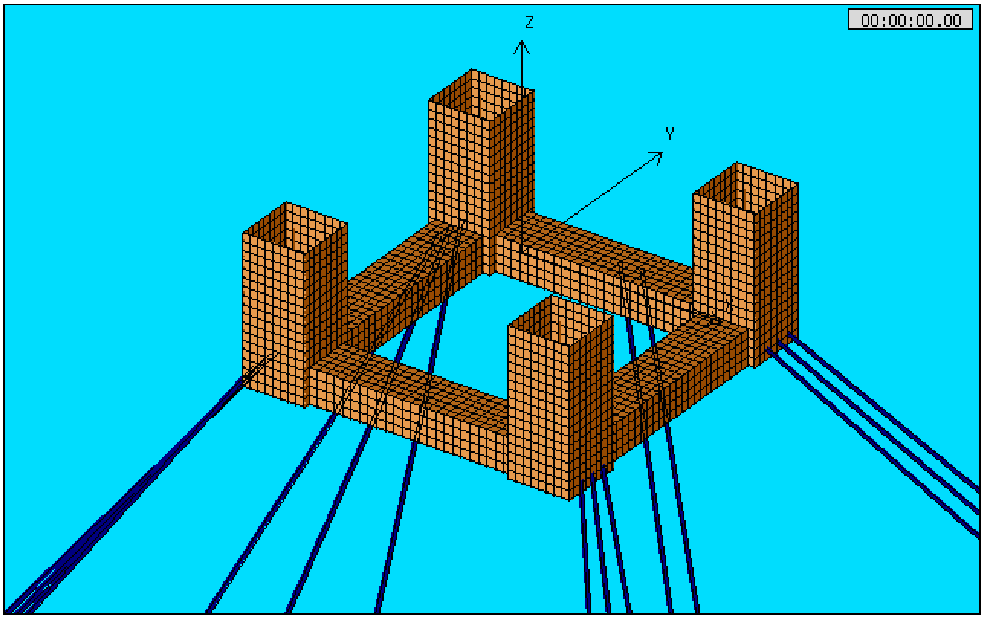

Figure 6: Generic Semi-Submersible Configuration [1]

A schematic description of the selected Semi-submersible locations for fatigue analysis is given in Figure 7 below. Based on the deterministic fatigue results, uncertainties were assigned to the random variables and these random variables were employed in a probabilistic fatigue analysis.

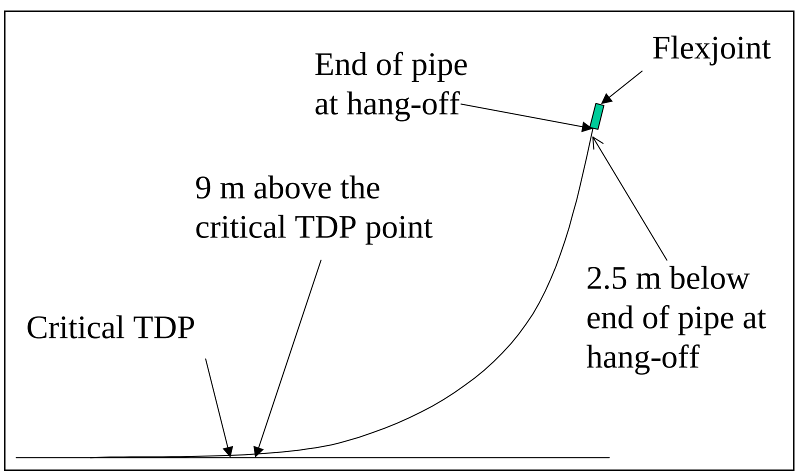

Figure 7: Selected Locations for SCR Reliability Analysis

3.2.2 Reliability Analysis

The total number of random variables employed in the analysis was 95. The description of the random variables is presented in the Table below.

Table 7: Description of Random Variables Used in the Reliability Analysis

Variable Name	Mean Value	Coefficient of Variation	Probability Distribution
DELTA	1.000	0.25	Weibull
BR	1.000	0.25	Weibull
BS	1.000	0.25	Lognormal
S-N_m	3.740	0.10	Lognormal
S-N_K	2.50E+13	0.10	Lognormal
Fatigue Stress Levels (MPa)	0.25-0.75 in 0.5 increments 1.5-59.5 in 1.0 increments 61-89 in 2.0 increments 94.0-97.0 in 3.0 increments 99.0 102-147 in 5.0 increments*	0.40	Gumbel

* The fatigue stress levels are based on deterministic results

A total of ten riser hot spot locations were selected for this analysis, grouped according to the following categories:

- Fully-Coupled Vessel Motion (FCVM)
    - Nominal Rotational Stiffness (NRS)
        - LC01: Critical Touch-Down Point (TDP)
        - LC02: 9m Above Critical TDP
        - LC03: End of Pipe at Hang-Off (EPHO)
        - LC04: 2.25m Below EPHO
- Un-Coupled Vessel Motion (UCVM)
    - Nominal Rotational Stiffness (NRS)
        - LC05: Critical Touch-Down Point (TDP)
        - LC06: 9m Above Critical TDP
        - LC07: End of Pipe at Hang-Off (EPHO)
        - LC08: 2.25m Below EPHO
    - Aging Rotational Stiffness (ARS)
        - LC09: End of Pipe at Hang-Off (EPHO)
        - LC10: 2.25m Below EPHO

Reliability analyses were carried out based on the First-Order Reliability Method (FORM), the results of which are presented below (please note the following abbreviations apply: FCVM = fully-coupled vessel motion; UCVM = un-coupled vessel motion; NRS = nominal rotational stiffness; ARS = aging rotational stiffness; TDP = touch-down point; EPHO = end of pipe at hang off).

Table 8: Probabilistic Analysis Results

Load Case ID	Description	Cumulative Damage	Reliability Index	Failure Probability
LC01	FCVM/NRS – Critical TDP	75.1E-06	4.047	25.9E-06
LC02	FCVM/NRS – 9m Above Critical TDP	67.3E-06	4.120	18.9E-06
LC03	FCVM/NRS – End of Pipe at Hang-Off	106.6E-06	3.850	59.0E-06
LC04	FCVM/NRS – 2.25m Below EPHO	38.3E-06	4.713	1.2E-06
LC05	UCVM/NRS – Critical TDP	115.2E-06	3.783	77.4E-06
LC06	UCVM/NRS – 9m Above Critical TDP	83.3E-06	3.922	43.8E-06
LC07	UCVM/NRS – End of Pipe at Hang-Off	72.5E-06	3.995	32.3E-06
LC08	UCVM/NRS – 2.25m Below EPHO	34.6E-06	4.789	0.8E-06
LC09	UCVM/ARS – End of Pipe at Hang-Off	110.1E-06	3.632	140.8E-06
LC10	UCVM/ARS – 2.25m Below EPHO	41.1E-06	4.573	2.4E-06

The results for all locations support INTEC's findings, suggesting locations 2.25m below EPHO are among the least critical in terms of fatigue, while TDP and EPHO locations are typically the most critical. It appears that reliability levels are higher near the critical TDP locations under fully coupled vessel motion, while reliability levels are greatest near the two EPHO locations under un-coupled vessel motion. Review of LC09 and LC10 suggest that reliability levels under nominal rotational stiffness (NRS) are significantly greater than those associated with aging rotational stiffness (ARS).

A review of the parametric importance factors predicted by the probabilistic analysis suggests that the relative influence or importance of uncertainty in the various parameters may be somewhat location dependent. Near the critical TDP locations, for example, the fatigue strength exponent (i.e., slope of the S-N curve) '*m*' and applied stress range 'S_i' are the two parameters whose uncertainty (indicated by their respective COVs) most affects riser reliability, followed the modeling uncertainty parameter B_R and Miner's index Δ (which generally exhibit an equal importance) and finally the bias factor B_S. Near the two hang-off locations, however, the importance of uncertainty in applied stress range becomes negligible. The pie charts in Figure 8 and Figure 9 show typical results for the distribution of parametric uncertainty importance.

As discussed in the previous case, the reliability and the relative importance of the basic random variables (B_R, Δ, B_S, m, K, and S_i) is strongly a function of the randomness of the fatigue strength exponent '*m*'. Therefore, efforts should be directed toward adequate calibration of 'm' for the various materials at the locations of interest. Since stress range S_i is a function of sea state statistics, close attention should also be paid to the calibration of this variable. Uncertainties in both '*m*' and 'S_i' will impact on the accuracy of both deterministic and probabilistic results.

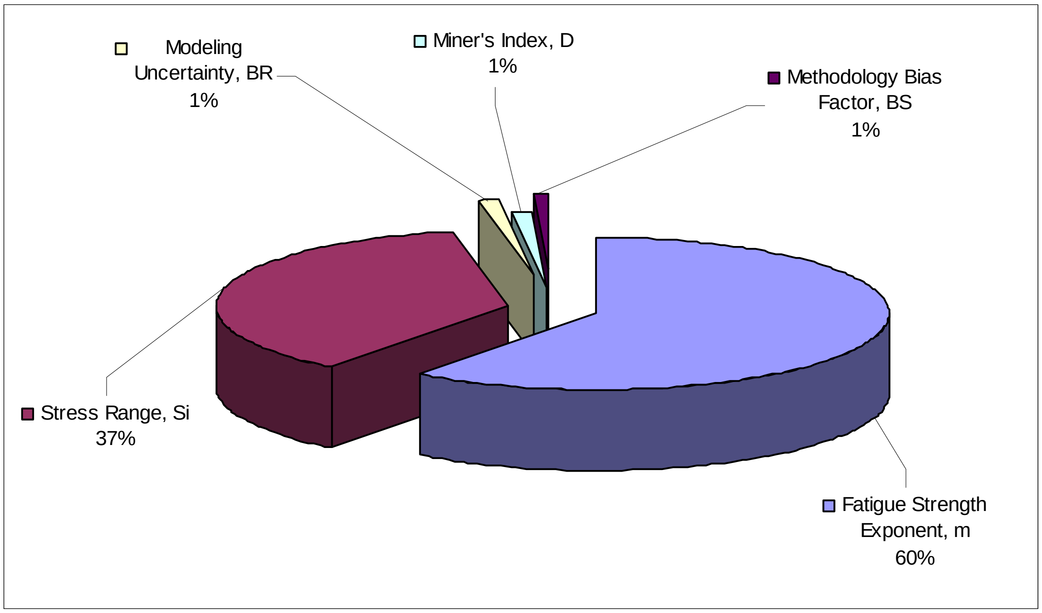

Figure 8: Distribution of Random Variable Importance Factors at TDP Locations

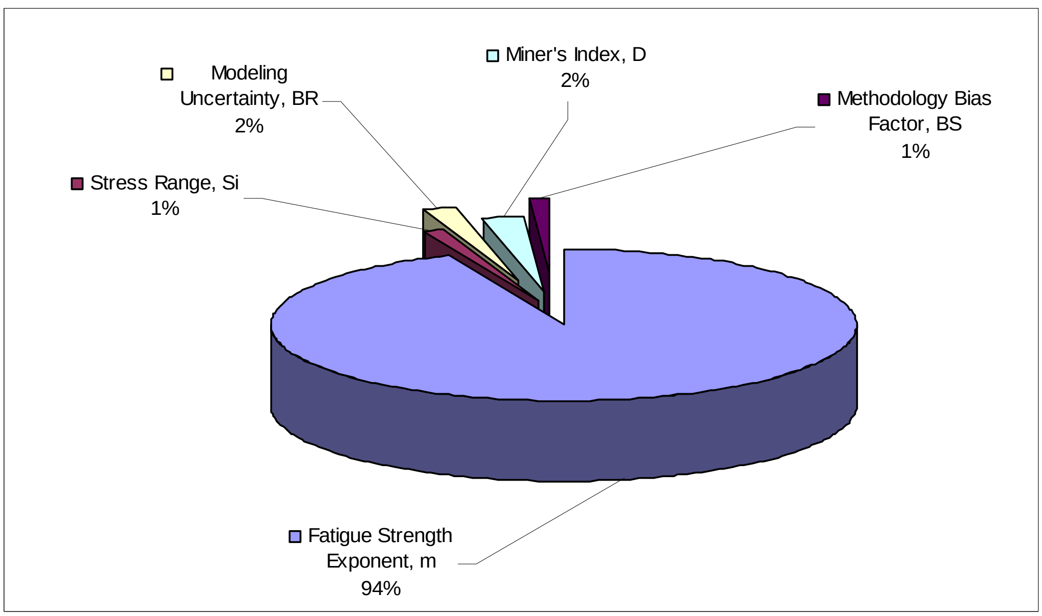

Figure 9: Distribution of Random Variable Importance Factors at EPHO Locations

To illustrate the parametric importance of the fatigue strength exponent ‘*m*’, a preliminary sensitivity study was conducted, in which its original probabilistic characteristics were modified and the resulting impact on reliability noted. The results are summarized in Figure 10, Figure 11 and Figure 12. The most critical hot-spot (see highlighted location in

Table 8) was selected for this demonstration.

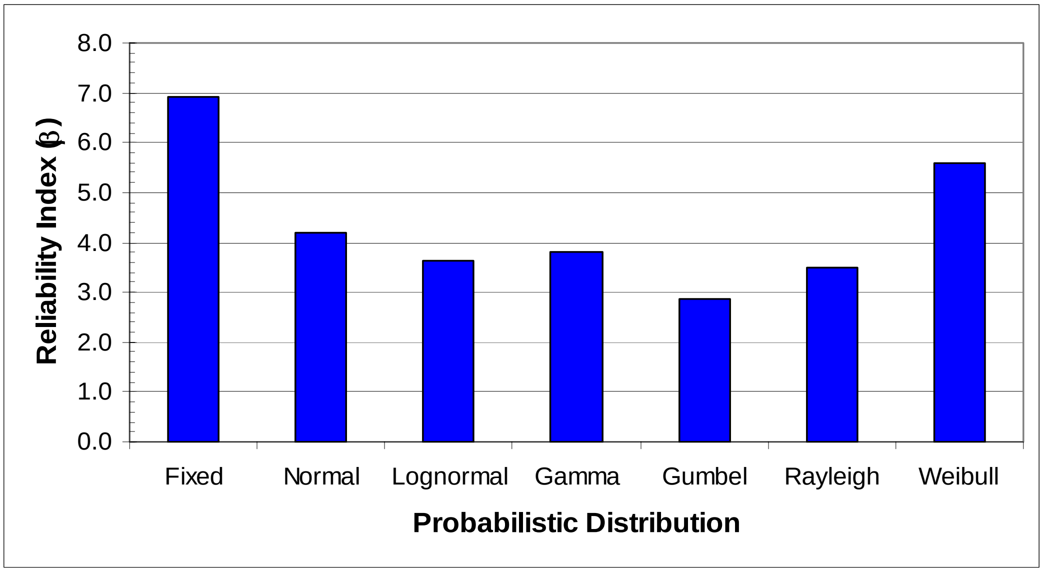

Figure 10: Reliability Index as a Function of Probabilistic Distribution of Fatigue Strength Exponent '*m*' (LC09 – EPHO)

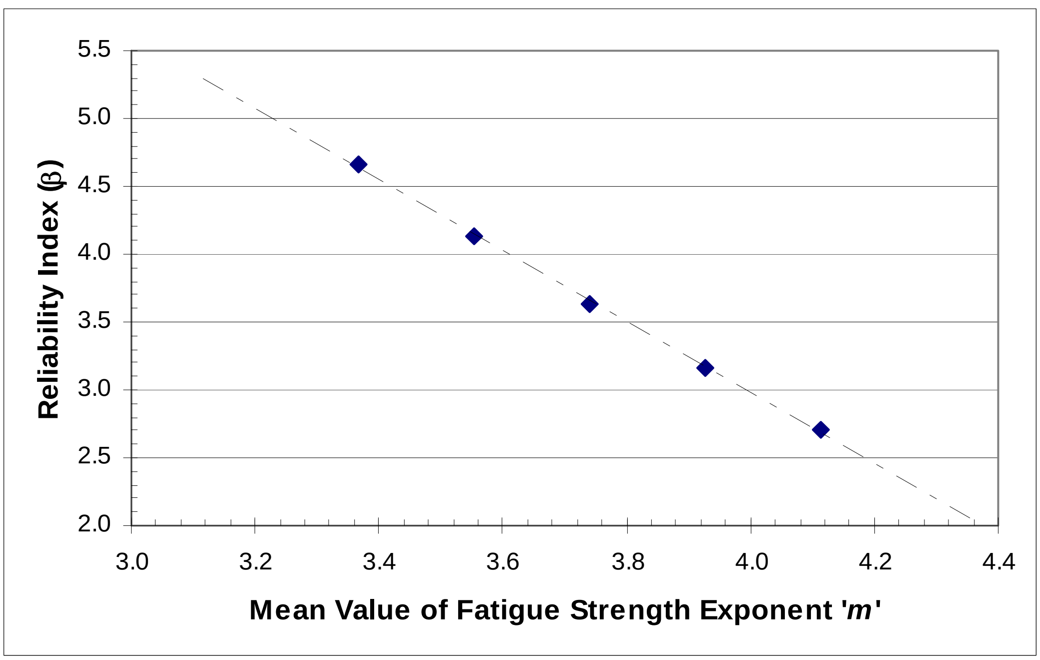

Figure 11: Reliability Index as a Function of Mean Value of Fatigue Strength Exponent '*m*' (LC09 – EPHO)

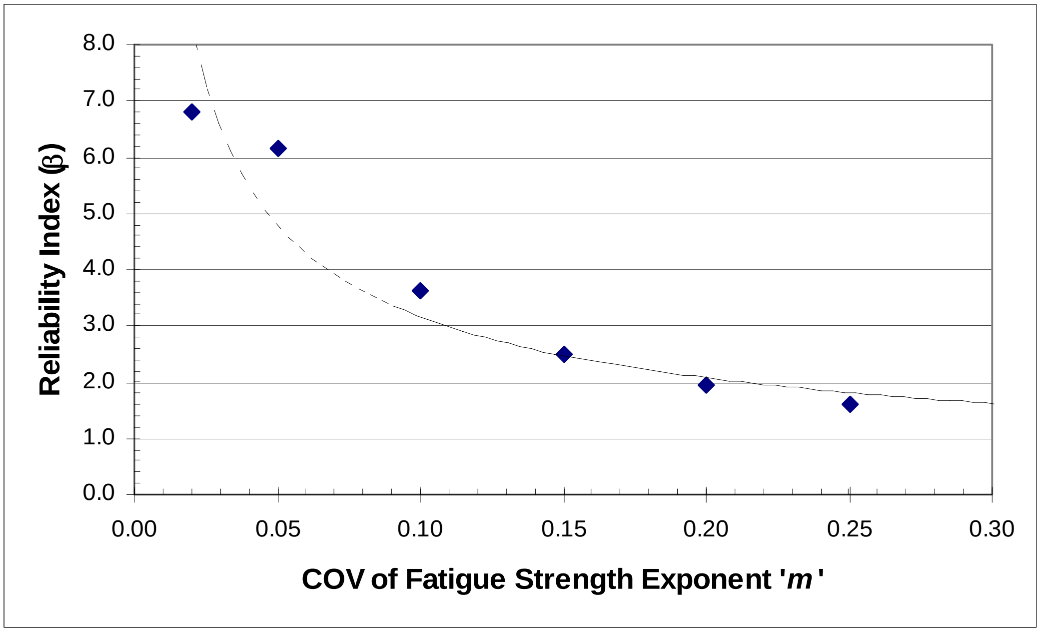

Figure 12: Reliability Index as a Function of COV of Fatigue Strength Exponent '*m*' (LC09 – EPHO)

3.3 Effect of Soil Pipe Interaction On Fatigue

3.3.1 Problem Description

Modeling approaches for soil reactions can result in significant variations in the predicted stresses of the steel catenary riser's pipe wall in the touchdown region. These stresses may govern fatigue and/or the extreme loading of the riser. The work is focused on comparisons made between conventional and advanced pipe-soil interaction model and the influence on predicted stress condition in the touchdown region of steel catenary risers. Limitations of the models and parameter sensitivities have been discussed in the companion report by INTEC Volume 1 [1]. This section is focused on using the deterministic fatigue result of the effect of the soil pipe interaction for probabilistic reliability assessment. As the fatigue response at the TDP is mainly driven by the vessel's heaves and heave's induced motions, the study concentrated on the semi-submersible platform, which poses more challenge in terms of motions affecting the TDP fatigue life.

3.3.2 Reliability Analysis Results

The total number of random variables used in the analysis was 63. The description of the random variables is presented in the Table 6 below.

Table 9: Description of Random Variables Used in the Reliability Analysis

Variable Name	Mean Value	Coefficient of Variation	Probability Distribution
DELTA	1.000	0.25	Weibull
BR	1.000	0.25	Weibull
BS	1.000	0.25	Lognormal
S-N_m	3.740	0.10	Lognormal
S-N_K	2.50E+13	0.10	Lognormal
Fatigue Stress Levels (MPa)	0.25-0.75 in 0.5 increments 1.5-55.5 in 1.0 increments*	0.40	Gumbel

* The fatigue stress levels are based on deterministic results

The analysis was performed for sea state 7 with 3 headings; Near (45^o), Far (135^o) and Cross (225^o). These are designated as, Sea State Near 7, Sea State Far 7 and Sea State Cross 7. Stress and cumulative damage results from both the conventional soil pipe model and Carisima trench model were used in the reliability analysis. All reliability analyses were carried out based on the First-Order Reliability Method (FORM), the results of which are presented in Table 10 and Table 11.

The results for all locations support INTEC's findings, suggesting that Sea Sate Near 7 location is the most critical in terms of fatigue, while Sea State Cross 7 location is typically the least critical. It appears that reliability levels for Carisima trench models are greater than those associated with conventional models. Thus the conventional models tend to be more conservative.

Table 10: Probabilistic Analysis Results (Conventional Model)

Load Case ID	Description	Cumulative Damage	Reliability Index	Failure Probability
LC001	Sea State Near 7	9.654E-03	1.764	38.9E-03
LC002	Sea State Far 7	7.546E-03	2.115	17.2E-03
LC003	Sea State Cross 7	6.491E-05	5.524	31.9E-09

Table 11: Probabilistic Analysis Results (Carisima Trench Model)

Load Case ID	Description	Cumulative Damage	Reliability Index	Failure Probability
LC004	Sea State Near 7	6.145E-03	2.229	12.9E-03
LC005	Sea State Far 7	2.833E-03	2.272	11.5E-03
LC006	Sea State Cross 7	8.179E-04	3.806	70.7E-06

The pie charts in Figure 13 and Figure 14 show typical results for the distribution of parametric uncertainty importance. The results from both the Conventional and Carisima models follow similar trends. In general, it is noted that, uncertainties in the fatigue strength exponent (i.e., slope of the S-N curve) '*m*' and the applied stress range, play a dominant role in reliability estimate and cannot be ignored in practice as is currently done.

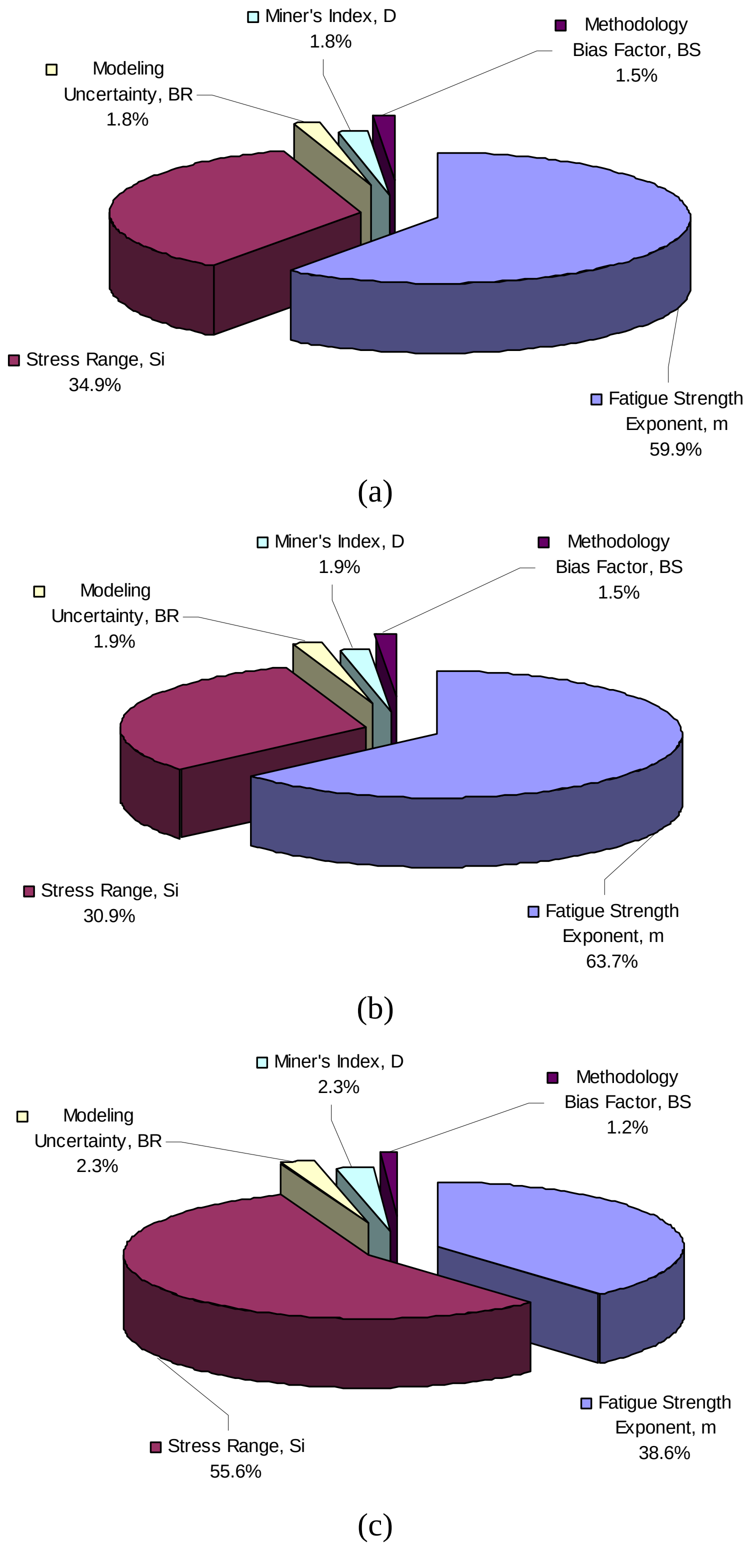

Figure 13: Distribution of Random Variable Importance Factors for Conventional Model (a) Near; (b) Far; and (c) Cross

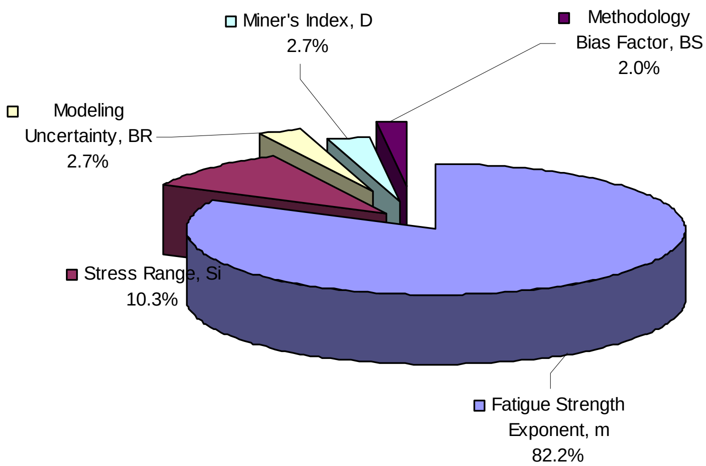

(a)

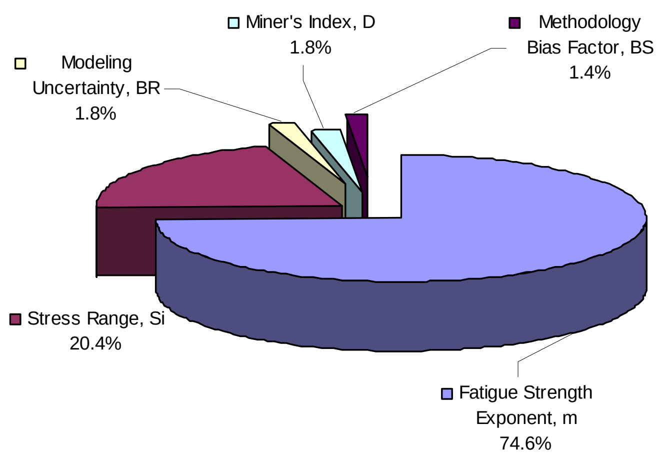

(b)

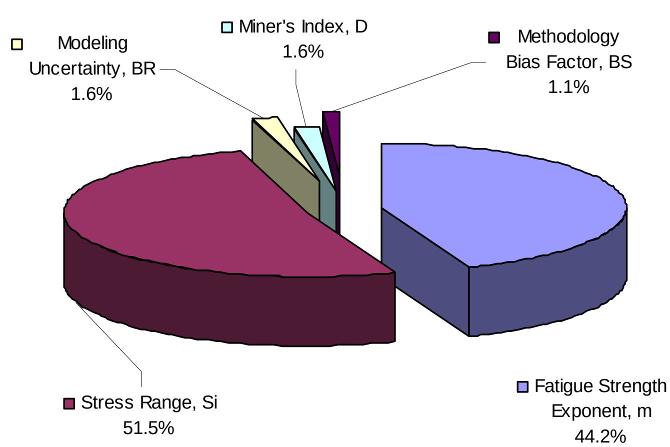

(c)

Figure 14: Distribution of Random Variable Importance Factors for Carisima Trench Model (a) near; (b) Far; and (c) Cross

4.0 SUMMARY, CONCLUSIONS AND RECOMMENDATIONS

4.1 SUMMARY AND CONCLUSIONS

The study developed and demonstrated a practical methodology and procedures for probabilistic reliability of SCR. A procedure for reliability assessment that uses deterministic fatigue results as the starting point in conjunction with reliability solution strategies such as first order reliability method was formulated and implemented for SCR. Three case studies that involve SPAR and semi-submersible SCR host structures were studied. The following conclusions can be drawn based on this study:

1. The methodology was constructed with careful consideration of the needs and practice offshore design procedures. It builds on deterministic results and should be seen as a complementary strategy to existing deterministic procedure for fatigue analysis.
2. This methodology realistically accounts for the various types/sources of uncertainties involved in the fatigue analysis of SCR including uncertainties in fatigue strength parameters, material types, as well as the fatigue loads. It should however be noted that uncertainties in the load and associated structural parameters were accounted for through a lump strategy. The lump strategy involves specifying maximum extreme load distribution (Gumbel) and high value of standard deviation for the structural response, namely stress levels, that is used in deterministic fatigue analysis.
3. The fatigue reliability methodology was applied to three case studies in which the SCR was attached to either a SPAR or semi-submersible platform. The case studies were used to investigate (a) the effect of hang-off strategies and riser tie-ins; (b) couples/uncoupled motion and the effect of flexible joint ageing on SCR hang-off; and (c) the effect of soil-pipe interaction. For case studies (a) and (b) the lowest reliability index for the selected critical locations was approximately 3.2. For case study (c) only one sea state was considered to assess the performance of the Conventional and Carisima models. In general, the reliability levels obtained from the Carisima model were higher than those from the conventional model. It should be noted that the reliability index is a measure of safety and a direct relationship exists between the reliability index and the probability of failure, with the probability of failure decreasing as the reliability index increases.
4. In general, the fatigue reliability estimates followed closely the trends of the deterministic results and this shows that the reliability strategy can complement existing deterministic efforts.
5. Most of the case studies that were investigated show in general uncertainty in fatigue strength exponent, *m*, has the highest impact on the fatigue reliability of SCR. It should be noted that although the probabilistic importance factor of *K* was low, in practice *K* and m are correlated random variables. This correlation was not considered in the current analysis. The second most important random variable is the stress range, S, which captures uncertainties in parameters, such as load, material properties.
6. Parametric sensitivity studies of the fatigue strength parameters indicate that the reliability is sensitive to both the standard deviation and probability distribution of this parameter, thus highlighting the need for accurate probability calibration of these random variables.

4.2 RECOMMENDATIONS

As stated above, the uncertainties in the loading and structural parameters were accounted for indirectly by assigning extreme random distributions to the stress levels. It is recommended that a strategy that directly assigns uncertainties to the primary loading and structural parameters be developed and the results be compared to those obtained in this study. Such an approach would involve the development of response surfaces using the various software products used for the deterministic analyses. It should be noted that such an approach would be more expensive compared to the approach presented in this study. However, it could serve to further validate the simplified approach adopted in this study.

In this study only the instantaneous reliability estimates have been presented. That is, the fatigue reliability at any instant in time is computed. The fact that the SCR had been in service and had survived prior to the particular instant has not been considered. In order to account for this, it is recommended that methodology for time dependent reliability of the SCR be developed. This would be useful for planning inspection and maintenance strategies for the SCR.

Since fatigue is a major concern for large diameter SCR for ultra deep water applications, it is further recommended that results of the current study and other related studies be compiled into a guidance document to provide best practices for SCR fatigue design and analysis.

5.0 REFERENCES

1. Probabilistic Reliability and Integrity Assessment of Large Diameter Steel Compliant Risers (SCR) for Ultra-Deepwater Operations: Volume 1: Main Study Report.

2. Hasofer, A.M. and Lind, N.C. (1974), "Exact and Invariant Second Moment Code Format," Proceedings of ASCE, Journal of the Engineering Mechanics Division, Vol. 100, No. EM1, pp.111-121.

3. Rackwitz, R. and Fiessler, B. (1978), "Structural Reliability Under Combined Random Load Sequences," Computers and Structures, Vol. 9, No. 5, pp.489-494.

4. Lui, P.L. and Der Kiureghian, A. (1991), "Optimization Algorithms for Structural Reliability," Structural Safety, Vol. 9, pp.161-177.

5. Orisamolu, I.R., Liu, Q. and Chernuka, M.W., (1992), "Probabilistic Reliability Analysis Using General Purpose Commercial Computer Programs, Technical Report No. TR-92-5, Martec Limited, Halifax.